

## **MODE I AND MIXED MODE NON-PRESCRIBED DISCRETE CRACK PROPAGATION IN CONCRETE**

J. Alfaiate and E. B. Pires  
Dept. Eng. Civil and Inst. Eng. de Estruturas, Território e Construção,  
Instituto Superior Técnico,  
Lisboa , Portugal

### **Abstract**

In this paper the finite element method is used to study non-prescribed crack propagation in concrete. Based on Hillerborg's discrete approach, cracks are allowed to evolve along interfaces or joints, with initial zero thickness. These interfaces are located along interelement boundaries of the finite element mesh which is kept unchanged during the analysis. Cracks open according to mode I fracture. Two different models are used for crack evolution: i) in the first model no shear stresses are allowed in the fracture zones; ii) in the second one aggregate interlock is taken into account. The results of two numerical examples are presented: a shear beam and a pull-out test. First these examples are analysed with the first model using both randomly generated and regular meshes with the purpose of evaluating the mesh independence of the results. Finally mixed mode fracture is considered for the shear beam test and the corresponding results are compared with the ones obtained from pure mode I analysis.

Key words: mixed mode, non-prescribed cracking, concrete

## 1 Introduction

In this paper non-prescribed crack propagation in concrete is dealt with. Hillerborg's discrete crack approach as well as the fracture energy concept are considered (Hillerborg et al. 1976). Cracks are allowed to evolve in a finite element mesh along fixed interfaces which are located along interelement boundaries. Since cracks open according to mode I fracture, the direction of the principal stress component  $\sigma_1$  is usually not perpendicular to the element boundaries. The misalignment between the fixed direction of the joint element in the mesh and the direction of mode I cracking is taken into account in such a way as to preserve the dissipation of energy along the correct crack paths. Crack evolution is modelled in two different ways. First, only pure mode I cracking is considered, i.e., cracks open and evolve according to mode I cracking. This means that no shear stresses are allowed in the fictitious cracks. In order to take aggregate interlock into consideration, mixed mode fracture is also considered. For this purpose, a multisurface plasticity model with a tension cut-off and a Coulomb friction law is introduced. These two limit surfaces evolve according to coupled tensile and shear softening rules. Although cracks still initiate perpendicularly to the direction of  $\sigma_1$ , shear stresses can develop within the fictitious cracks after their initiation.

The results of two numerical examples are presented: a shear beam and a pullout test. First a pure mode I analysis is performed with regular and irregular meshes in order to evaluate the mesh independence of the model. Finally mixed mode fracture is considered for the shear beam and the corresponding results are compared with the results obtained from pure mode I analysis.

## 2 Material Model

In this Section the constitutive relationships adopted for concrete are presented. Two different regions within the material can be distinguished: i) the bulk, corresponding to the continuum and ii) the fracture zones, corresponding to microcracking of concrete. A linear-elastic isotropic constitutive relation is adopted to describe the behaviour of the non-fractured zones of the material. In tension, softening is initiated when the stresses attain a limit strength curve corresponding to Rankine's criterion: the resistance of the material is limited to the uniaxial tensile strength  $f_t$ .

In the fracture zones the cracks are allowed to develop according to Hillerborg's fictitious crack approach. Softening is described, in each point of the fictitious cracks, by stress-relative displacement relationships. Mode I and mode II fracture energies are assumed to be material properties.

## 2.1 Pure mode I analysis

In pure mode I analysis the bilinear relationship between the stress normal to the fictitious crack and the relative crack opening displacement introduced by Petersson (1981) is adopted. Mode I fracture is assumed for the initiation and evolution of a fictitious crack: the crack paths are perpendicular to the direction of the maximum principal stress  $\sigma_I$ . Due to this assumption, the principal stress directions do not vary after initiation of a crack since no shear stresses are allowed at the fracture zones.

## 2.2 Mixed mode analysis

In order to consider mixed mode fracture, a modified version of Lourenço and Rots's multisurface plasticity model is adopted (Lourenço and Rots 1997). In the fracture zone, or fictitious crack, two directions can be defined: the normal direction which corresponds to the direction of  $\sigma_I$ , and the tangential direction, parallel to the crack faces. For each direction a stress vector component and a relative displacement vector component are defined. The horizontal axis in fig.1 represents the normal stress acting at the fictitious crack and the vertical axis represents the tangential stress. In this two dimensional stress space, two limit surfaces are adopted: a tension cut-off limit surface for mode I failure and a Coulomb friction envelope for mode II failure. The cut-off mode I failure is initially characterised by the tensile strength of concrete  $f_t$ . The Coulomb friction envelope is initially characterised by the cohesion coefficient  $c_0$  and by the internal friction angle  $\phi$ . Both yield functions follow exponential softening flow rules.

The tension mode yield function is given by:

$$f_n(\sigma_n, \kappa_n) = \sigma_n - f_t \exp\left(-\frac{f_t}{G_F} \kappa_n\right) \quad (3)$$

where  $\sigma_n$  is the normal stress vector component measured in the fictitious crack and  $\kappa_n$  is a scalar parameter which controls the amount of softening. We take  $\kappa_n = w_n^p$ , where  $w_n^p$  is the plastic normal relative displacement. The yield surface given in (3) is allowed to evolve along the direction of  $w_n^p$  (associated flow rule).

The shear mode yield function is given by:

$$f_s(\sigma_n, \sigma_s, \kappa_s) = |\sigma_s| + \sigma_n \tan\phi - c_0 \exp\left(-\frac{c_0}{G_F^{II}} \kappa_s\right) \quad (4)$$

where  $\sigma_s$  is the tangential stress vector component measured in the fictitious crack,  $G_F^{II}$  is the mode II fracture energy and  $\kappa_s$  is a scalar parameter that controls the amount of softening. In this case,  $\kappa_s = w_s^p$ , where  $w_s^p$  is the plastic relative shear displacement. A non-associated flow rule is adopted with a plastic potential  $g_s$  given by:

$$g_s(\sigma_n, \sigma_s, \psi) = |\sigma_s| + \sigma_n \tan \psi - c_0 \quad (5)$$

where  $\psi$  is the dilatancy angle.

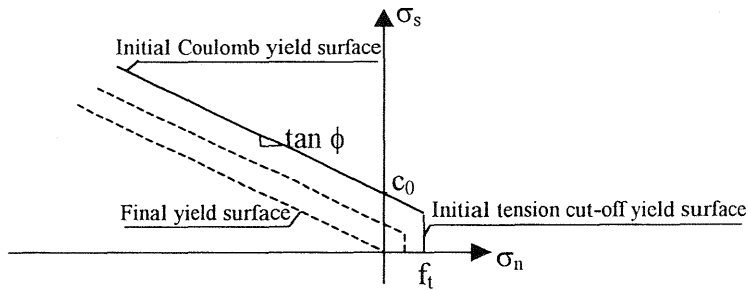


Figure 1. Yield surfaces

An isotropic softening criterion is assumed, i.e., both yield surfaces shrink the same relative amount in the stress space, and both keep the origin (see fig.1).

### 3 Numerical Implementation

The finite element method is used in the numerical analysis. The continuum is discretised by means of isoparametric 4 node elements whereas linear interface elements are used to represent the fictitious cracks within the material. A trapezoidal rule is used to integrate the interface elements, with the integration points located at the nodes.

In the examples presented, the crack paths are not known in advance. If mode I is assumed, the location of the fictitious cracks should always be perpendicular to the directions of the maximum principal tensile stress  $\sigma_I$ . One solution consists of aligning the interface elements with the directions of the fictitious cracks (Ingraffea et al. 1985, Carpinteri et al. 1989). Here a different approach is presented where no remeshing is necessary during the analysis. Interface elements are located, from the beginning, along the boundaries of the continuum elements within zones where cracks are expected to occur. Once the mesh is defined it remains unchanged during the whole analysis. An evolution algorithm is introduced which takes into account the misalignment between the direction perpendicular to  $\sigma_I$  and the direction of the interfaces in the mesh. Interface elements at the crack tip are connected and their properties are projected onto an approximate crack direction, close to the direction perpendicular to  $\sigma_I$  (Alfaiate et al. 1997).

The response of the structure is evaluated incrementally and, for each step, the following procedures are followed:

1. Evaluation of the incremental structure stiffness  $\mathbf{K}_t$ ;
2. Solution of the system of equations  $\mathbf{K}_t \Delta \mathbf{u} = \Delta \lambda \mathbf{F}$ , where  $\Delta \mathbf{u}$  is the vector of incremental displacements,  $\Delta \lambda$  is the step size and  $\mathbf{F}$  is the vector of nodal forces;
3. Determination of the internal forces  $\mathbf{F}_i$ . The Newton-Raphson and the arc-length methods are used to obtain convergence. If equilibrium is not attained a new iteration is performed; otherwise we go to step 4; if no convergence is achieved after a given number of iterations, a smaller step is tried;
4. Evaluation of the values of the total variables and return to 1.

For the tests presented, a monotonic increasing opening of a main fictitious crack is imposed. The step size  $\Delta \lambda$  is controlled such that the following equation is satisfied:

$$\frac{\Delta \lambda^2}{\Delta \lambda_0^2} + \frac{|\Delta \mathbf{u}_c|^2}{|\Delta \mathbf{u}_{c0}|^2} = 2.0 \quad (6)$$

where  $\Delta \lambda_0$  is the initially prescribed step size,  $\Delta \mathbf{u}_c$  are the incremental displacements measured at the nodes belonging to the crack faces and  $\Delta \mathbf{u}_{c0}$  are the incremental displacements obtained at the tip of the first fictitious crack as soon as it opens.

In each iteration the arc-length method is used and the following constraint equation is imposed:

$$\Delta w_{\text{tip}} = \Delta w_{\text{tip},1} \quad (7)$$

where  $\Delta w_{\text{tip}}$  is the incremental relative displacement measured at the crack tip along the approximate direction of  $\sigma_I$  and  $\Delta w_{\text{tip},1}$  is equal to the  $\Delta w_{\text{tip}}$  obtained in the first iteration. In this way, the same amount of incremental relative displacement at the crack tip is enforced in each iteration. Note that  $\Delta w_{\text{tip}}$  takes into account the connection between two interface elements  $i$  and  $j$  at the crack tip according to:

$$\Delta w_{\text{tip}} = \frac{\Delta s_i \Delta w_i + \Delta s_j \Delta w_j}{\Delta s_i + \Delta s_j} \quad (8)$$

where  $\Delta w_i$  and  $\Delta w_j$  are the incremental relative displacements obtained from interfaces  $i$  and  $j$  at the crack tip, respectively, and  $\Delta s_i$  and  $\Delta s_j$  are line segments along both interfaces, which are equal to half the length of the elements. At the beginning of each step the tangent stiffness matrix is evaluated. During the following iterations the tangent stiffness matrix  $\mathbf{K}_t$  is

kept unchanged unless at least one fictitious crack experiences modifications such as: the constitutive relation changes from mode I to mixed mode or from unloading to mode I.

## 4 Numerical tests

In this Section two different numerical tests are presented: a shear beam and a pullout test.

The former consists of a simply supported notched beam subjected to shear. A plane stress state is assumed. Ingraffea (1989) performed several experiments with this beam. The control parameter adopted in the experimental tests and in the computations is the monotonic opening of the crack mouth sliding displacement (CMSD); the crack mouth refers to the lowest part of the notch and the sliding displacement refers to the relative displacement measured along the vertical direction between notch faces (see fig.2).

The second test consists of the pullout of an embedded steel disk from a concrete specimen. The pullout of the steel disk is made against a steel reaction ring (see fig. 4). The disk is assumed to be completely disconnected from the surrounding concrete, except for the upper surface of the disk where full contact is assumed. The stem is not modelled in the finite element mesh: a uniform stress distribution is applied to the central part of the upper surface of the disk which corresponds to the stem. A monotonic increasing upward displacement of the disk is enforced in the numerical analysis. This is an axisymmetric test and therefore only half of the specimen is shown in fig. 4.

### 4.1 Pure mode I analysis

First, the two tests are submitted to a pure mode I analysis: the fictitious cracks initiate and evolve in mode I. The results presented in this Section are obtained with two different meshes. For each test an irregular mesh is obtained from a regular one with the nodes randomly located within the neighbourhood of their initial positions. This neighbourhood consists of a circle centered at each initial nodal position and with a diameter equal to 20% of the maximum side length of the rectangular elements which share that node. In figs.2 and 4 the deformed irregular meshes obtained for the shear beam and the pullout test are shown. The experimental results obtained by Ingraffea lie in the shadowed region shown in fig.3. In this figure the load-CMSD curves obtained numerically with our model, with the regular mesh and the irregular mesh, are also presented. From fig.3 we conclude that the maximum load obtained with the present model is smaller than the experimental one. A better approximation of the experimental maximum load was obtained by Ingraffea (1989) using a discrete approach

with remeshing and considering aggregate interlock. From figs. 3 and 5 we conclude that, in both tests, no significant mesh dependence is observed.

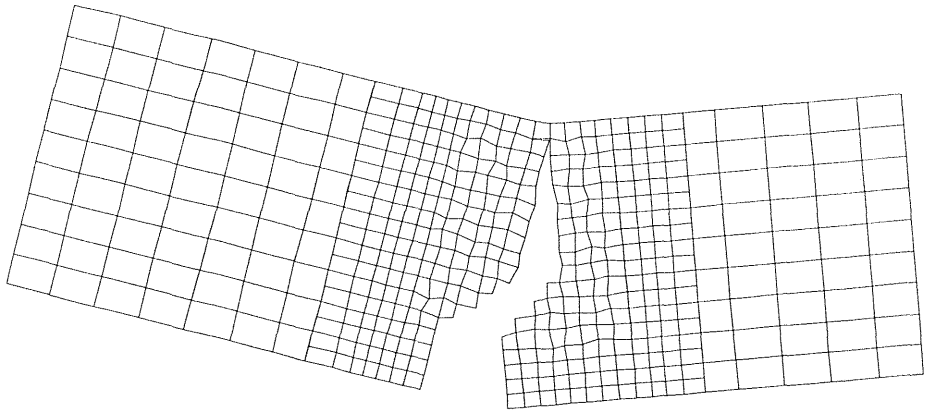


Figure 2. Deformed mesh obtained for the shear beam: irregular mesh

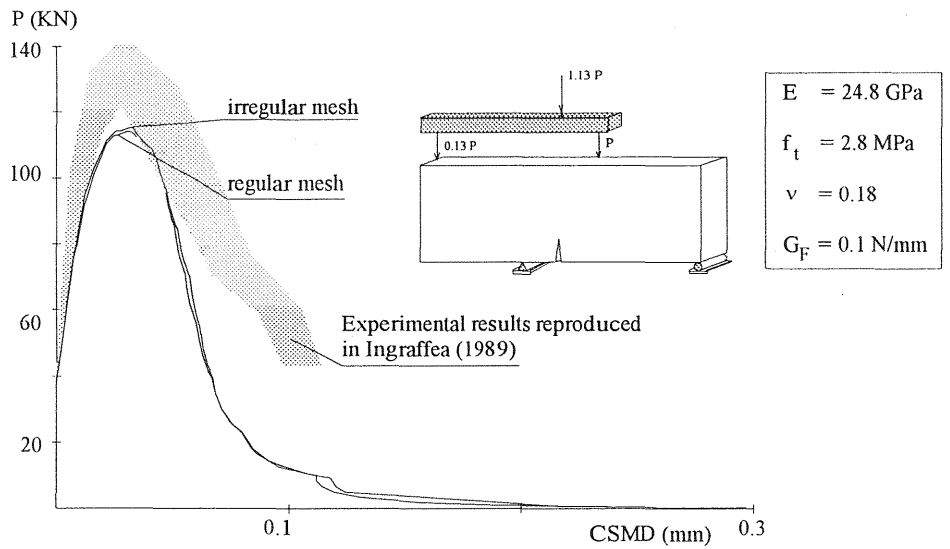


Figure 3. Load-CMSD curves obtained by Ingraffea (experimentally) and with the present model

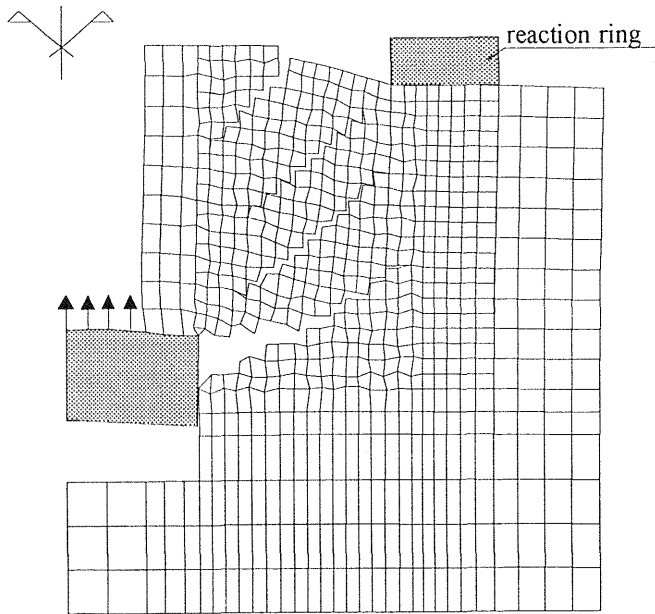


Figure 4. Deformed mesh obtained from the pullout test: irregular mesh

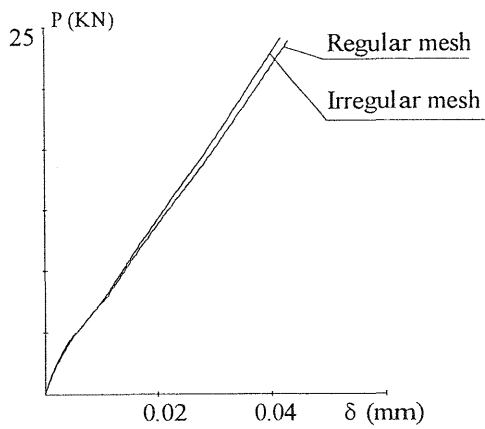


Figure 5. Pullout test: P- $\delta$  curves obtained with the present model

#### 4.2 Mixed mode analysis

The shear beam is also analysed with the multisurface plasticity model mentioned in Section 2.2. The material parameters adopted are:  $f_t = 2.8$  MPa;  $c_0 = f_t$ ;  $G_F = 0.1$  N/mm;  $G_F^{II} = G_F$ ;  $\phi = 30^\circ$ ;  $\psi = 0^\circ$ . The maximum shear stress with no confinement is assumed to be smaller than  $f_t$  (Walraven (1980) recommends a value of  $2/3f_t$ ). However, in order to stress the im-

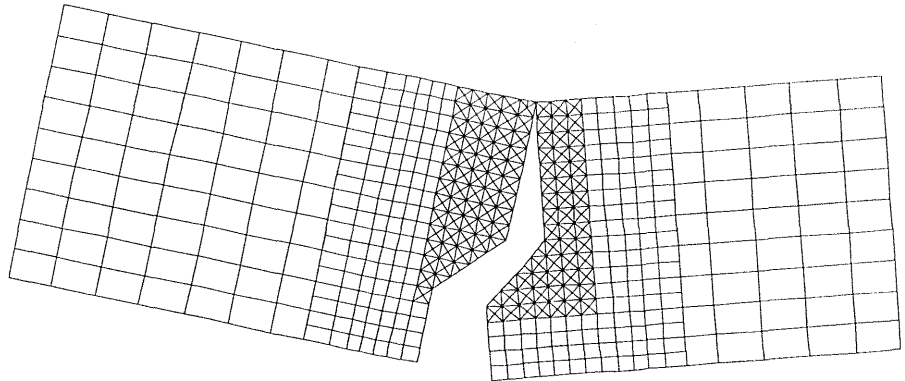


Figure 6. Deformed mesh obtained with aggregate interlock

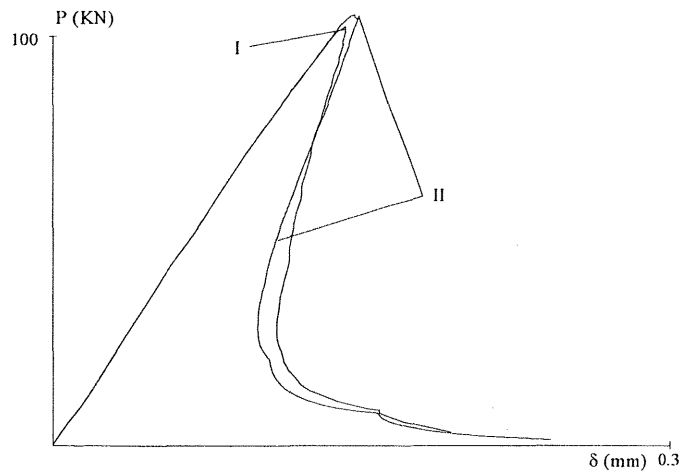


Figure 7. P- $\delta$  curves obtained without (I) and with (II) aggregate interlock

portance of aggregate interlock, a value of  $c_0$  equal to  $f_t$  is adopted. In fig.6 the deformed mesh obtained near the formation of a mechanism is shown. In fig.7 both mode I (I) and mixed mode (II) load displacement (P- $\delta$ ) curves are presented. From this figure it can be seen that, in this test, approxi-

mately the same value for the peak load is obtained with both i) the mode I model and ii) the mixed mode model with the material parameters adopted.

## 5 Conclusions

Two main conclusions can be drawn from these numerical tests:

- i) no significant mesh dependence is observed with the algorithm proposed for non-prescribed crack propagation in concrete;
- ii) with both models proposed and for the shear beam, mixed mode analysis and pure mode I analysis lead to approximately the same value for the peak load.

## 6 References

- Alfaiate J., Pires, E.B. and Martins, J.A.C. (1997), A Finite Element Analysis of Non-Prescribed Crack Propagation in Concrete, **Computers & Structures**, 63, 1, 17-26.
- Carpinteri A., Valente S., Bocca P. (1989), Mixed mode cohesive crack propagation, in **Proc. 7th Conf. On Fracture (ICF-7)**, Eds. K. Salama, K. Ravi-Chandar, D.M.R. Taplin, P. Rama Rao, Pergamon Press, 2243-2257.
- Hillerborg A., Modeer, M. and Petersson, P.E. (1976), Analysis of crack formation and crack growth in concrete by means of fracture mechanics and finite elements, in **Cem. And Concr. Res.** , 6, 783-792.
- Ingraffea, A., Saouma V. (1985), Numerical modelling of discrete crack propagation in reinforced and plain concrete, in **Engineering Application of Fracture Mechanics**, (edited by George C. Sih and A. DiTommaso), Martinus Nijhoff Publishers.
- Ingraffea A. (1989), Shear cracks, Fracture Mechanics of Concrete Structures - from theory to applications, **Report of the Technical Committee 90-FMA Fracture Mechanics of Concrete - Applications**, (edited by L. Elfgren, Chapman and Hall), 231-233, London, U.K..
- Lourenço, P.B., Rots, J.G. (1997), A multi-surface interface model for the analysis of masonry structures, **J. Engrg. Mech.**, ASCE, 123(7), 660-668.
- Petersson P.-E. (1981), **Crack growth and development of fracture zones in plain concrete and similar materials**, Report TVBM-1006, Div. of Building Materials, Lund Inst. of Technology, Sweden.
- Walraven, J.C. (1980), **Aggregate Interlock: A theoretical and experimental analysis**, Delft University press, Delft University of Technology, Delft, The Netherlands.